# Introduction of ORF3a-Q57H SARS-CoV-2 Variant Causing Fourth Epidemic Wave of COVID-19, Hong Kong, China

Daniel K.W. Chu,[1] Kenrie P.Y. Hui,[1] Haogao Gu, Ronald L.W. Ko, Pavithra Krishnan, Daisy Y.M. Ng, Gigi Y.Z. Liu, Carrie K.C. Wan, Man-Chun Cheung, Ka-Chun Ng, John M. Nicholls, Dominic N.C. Tsang, Malik Peiris, Michael C.W. Chan, Leo L.M. Poon

We describe an introduction of clade GH severe acute respiratory syndrome coronavirus 2 causing a fourth wave of coronavirus disease in Hong Kong. The virus has an ORF3a-Q57H mutation, causing truncation of ORF3b. This virus evades induction of cytokine, chemokine, and interferon-stimulated gene expression in primary human respiratory cells.

Hong Kong, China, has had 4 waves of coronavirus disease (COVID-19) outbreaks since the emergence of severe acute respiratory syndrome coronavirus 2 (SARS-CoV-2) in December 2019. By February 1, 2021, Hong Kong had recorded 10,453 reverse transcription PCR (RT-PCR)–confirmed COVID-19 cases, and many of those occurred during the last 2 waves. The third wave occurred during late June to early September 2020 and was caused by a single introduction of GISAID (https://platform.gisaid.org) clade GR virus (*1*). The fourth wave began in early November 2020 and was caused by a newly introduced GISAID clade GH SARS-CoV-2 (*1*). We describe the origin of a clade GH virus causing the fourth epidemic wave in Hong Kong.

## The Study

Before our investigation, epidemiologic investigations in early October 2020 revealed 2 local COVID-19 clusters associated with bar/building X or hotel C (Appendix Figure 1, https://wwwnc.cdc.gov/EID/article/27/5/21-0015-App1.pdf), both of which are located in the same district of Hong Kong. The bar/building X cluster had 15 RT-PCR–confirmed COVID-19 cases (patients BB1–BB15), and the hotel C cluster had 9 RT-PCR–confirmed cases (patients C1–C9) (Figure 1).

To determine whether the 2 clusters were epidemiologically linked, we sequenced near full-length genomes from all available samples, including respiratory samples from patients BB1–BB13 and patients C1–C9, by using a previously described protocol (*2*,*3*). We found the viral genomes were highly similar (sequence identity ≥99.98%) (Appendix Figure 2). All sequences belonged to clade GH, which was not found in local COVID-19 cases during the third wave (*1*). Our results indicate that this newly introduced clade GH virus was circulating in the local community ≈1 month before the beginning of the fourth epidemic wave in Hong Kong.

We also noted 4 imported cases (patients A1–A4) in a nearby hotel (hotel A), which is ≈350 m walking distance from bar/building X and hotel C, during late September to early October 2020 (Figure 1; Appendix Table 1). Patients A1–A3 traveled from Nepal to Hong Kong on the same direct flight and had their mandatory quarantine in hotel A during September 9–20, 2020 (Appendix). Of note, 2 additional RT-PCR–confirmed cases, patients B1 and B2, traveled on the same flight as patients A1–A3 (Figure 1). B1 and B2 were unrelated to patients A1–A3 and had their mandatory quarantine in hotel B, which is in another district of Hong Kong. Our sequencing results indicate that the viral genomes of these 5 cases are identical or almost identical to those from the 2 local clusters (Appendix

Author affiliations: The University of Hong Kong, Hong Kong, China (D.K.W. Chu, K.P.Y. Hui, H. Gu, R.L.W. Ko, P. Krishnan, D.Y.M. Ng, G.Y.Z. Liu, C.K.C. Wan, M.-C. Cheung, K.-C. Ng, J.M. Nicholls, M. Peiris, M.C.W. Chan, L.L.M. Poon); Department of Health, Hong Kong (D.N.C. Tsang)

DOI: https://doi.org/10.3201/eid2705.210015

[1]These first authors contributed equally to this article.

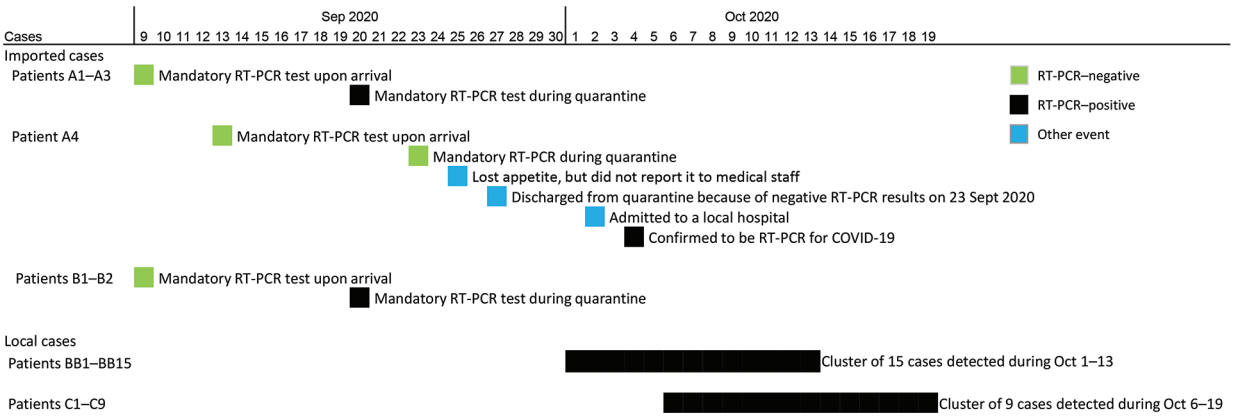


**Figure 1.** Timeline of COVID-19 cases during fourth epidemic, September 9–October 19, 2020, Hong Kong, China. Asymptomatic cases occurred in patients A1–A3, B1, B2, BB4, BB12, BB13, BB15, C3, C4, C7, and C9. Symptomatic cases occurred among patients A4, BB1–BB3, BB5–BB11, BB14, C1, C2, C5, C6, and C8. COVID-19, coronavirus disease; RT-PCR, reverse transcription PCR.

Figure 2). Although it is not known whether in-flight transmission occurred among patients A1–A3 and B1 and B2 (*2*), our results suggest that the fourth COVID-19 epidemic wave in Hong Kong was introduced from Nepal, and the deduced sequences are closely related to sequences from Nepal (Appendix Figure 2).

Patient A4, who was quarantined in hotel A during September 13–27, 2020, also traveled from Nepal to Hong Kong on a separate flight. The viral genome of case A4 is identical or closely related to sequences from patients A1–A3 and B1 and B2. Patient A4 had consecutive negative RT-PCR results upon arrival and on day 12 during quarantine (Figure 1). Patient A4 might have acquired SARS-CoV-2 in Nepal and had a long incubation period. Alternatively, A4 might have acquired the infection while quarantined in hotel A. We do not know how this virus was introduced into the local community. However, patient A4 finished the mandatory quarantine on September 27 and started to interact with the local community 7 days before testing positive for SARS-CoV-2. Patient A4 might have had opportunities to introduce the clade GH virus into the local community, but we cannot exclude the possibility that this virus was introduced in hotel A via an unnoticed transmission chain or chains.

Our full genome analysis revealed that the wave 4 virus has several nonsilent mutations associated with host adaptation (*4*–*6*; B. Zhou et al., unpub. data, https://doi.org/10.1101/2020.10.27.357558), including mutations in the RNA-dependent RNA polymerase (RdRp[L323P]), Spike(D614G), open reading frame 3a (ORF3a[Q57H]), ORF3b(E14*), and nucleocapsid (N[S194L]) proteins. The ORF3a(Q57H) mutation leads a major truncation of ORF3b protein, ORF3b(E14*) (*6*). Because the ORF3b protein is reported to be a potent interferon antagonist (*6*), we isolated the virus from patient A2 and conducted phenotypic characterizations using ex vivo human organ cultures and human airway organoids (*7*,*8*). We noted that this wave 4 virus contains a Spike(D614G) mutation that is associated with enhanced virus replication and transmission (B. Zhou et al., unpub. data). To differentiate the effect of Spike(D614G) and ORF3a(Q57H) mutations in our assays, we included viruses isolated from epidemic waves 1 and 3 as controls. The wave 1 virus we studied did not have these 2 mutations; the wave 3 virus had the Spike(D614G) but not the ORF3a(Q57H) mutation (Table). Our sequence data are available from GISAID (accession nos. EPI_ISL_760031–58).

We first studied the virus replication kinetics by using human bronchus and lung ex vivo cultures (Appendix Figure 3). In bronchus tissues, the wave 4 virus had a replication rate comparable to the wave 1 virus, but it had a lower replication rate than the wave 1 virus in lung tissues at 48 h, 72 h, and 96 h and a lower area under the curve. By contrast, the wave 3 virus had a slightly higher replication rate than the wave 1 virus in human bronchus, but not in human lung ex vivo cultures (Appendix Figure 3, panel A). Immunohistochemical staining analyses confirmed these observations (Appendix Figure 3, panel B). We found the wave 3 virus, not the wave 4 virus, might have marginally better replication competence than the wave 1 virus.

We previously demonstrated that the wave 1 virus is not a potent proinflammatory cytokine and chemokine inducer in infected human cells (*7*). To determine whether the ORF3a(Q57H) would affect this phenotype, we tested these viruses in human

**Table.** Amino acid differences between severe acute respiratory syndrome coronavirus 2 variants in 3 waves of coronavirus disease, Hong Kong, China*

| Genome category | Amino acid position | Wave 1 virus VM20001061 | Wave 3 virus Case 4533 | Wave 4 virus Patient A2 |
|---|---|---|---|---|
| ORF1A/1AB | | | | |
| NSP2 | 141 | M | **V** | M |
| NSP3 | 85 | A | **V** | A |
| | 238 | V | V | **L** |
| | 453 | V | **I** | V |
| | 1,179 | A | A | **V** |
| RdRp | 323 | **P** | L | L |
| EndoRNAse | 231 | A | **V** | A |
| Spike | 12 | S | **F** | S |
| | 25 | **L** | P | P |
| | 367 | **F** | V | V |
| | 614 | **D** | G | G |
| | 680 | **Q** | R | R |
| | 1,002 | **E** | Q | Q |
| ORF3a | 57 | Q | Q | **H** |
| | 227 | T | T | **I** |
| ORF3b | 14 | E | E | STOP |
| ORF8 | 62 | **L** | V | V |
| | 84 | S | L | L |
| Nucleocapsid | 12 | A | **G** | A |
| | 194 | S | S | L |
| | 203 | R | **K** | R |
| | 204 | G | **R** | G |
| ORF9b | 9 | H | **D** | H |

*Bold text indicates position where isolated differs from the other isolates. A, alanine; D, aspartic acid; E, envelope; F, phenylalanine; G, glycine; H, histidine; I, isoleucine; L, leucine; M, membrane; NSP, nonstructural protein; ORF, open reading frame; P, proline; Q, glutamine; R, arginine; S, spike; STOP, stop codon; T, threonine; V, valine.

respiratory organoid cultures. We extracted RNA from infected organoids at 48 h post infection and tested the RNA samples in RT-PCR assays for a range of innate immune response genes. The viral RNA in organoids infected by the wave 3 or 4 virus was ≈1 log unit lower than the one infected by the wave 1 virus ($p<0.05$; Figure 2). The cytokine, chemokine, and interferon-stimulated gene mRNA levels induced by

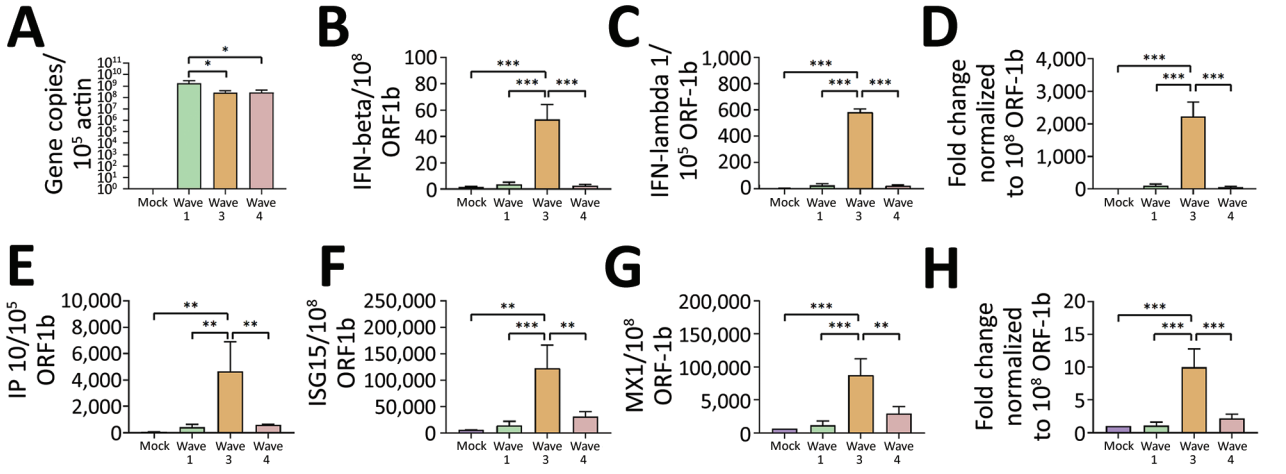


**Figure 2.** Innate immune responses in human airway organs experimentally infected with SARS-CoV-2 viruses from COVID-19 epidemic waves 1, 3, and 4, Hong Kong, China. A) ORF1b; B) IFN-β; C) IFN-λ 1; D) IFN-λ 2/3; E) IP-10; F) ISG15; G) MX1; H) MDA5. Messenger RNA expression of viral genes in human airway air-liquid interface organoids (n = 4; multiplicity of infection = 2) from the apical side at 48 h post infection. Mock samples were not infected. The gene expression of infected cells was first normalized with β-actin and further normalized with ORF1b gene. The gene expression of mock-infected cells was presented after normalization with β-actin. The differences were compared using 1-way ANOVA followed by a Tukey multiple-comparison test. Means and SD error bars are as shown. *p<0.05; **p<0.01; ***p<0.001. COVID-19, coronavirus disease; IFN, interferon; IP-10 interferon gamma-induced protein-10; ISG15, interferon stimulated gene 15; MDA5, melanoma differentiation-associated protein 5; MX1, interferon-induced GTP binding protein 1; ORF, open reading frame; SARS-CoV-2, severe acute respiratory syndrome coronavirus 2.

the wave 4 virus were low and were only similar to the wave 1 virus. In addition, gene expressions in cells infected by the wave 3 virus were much higher than those caused by the wave 1 virus. Interferon gamma-induced protein-10 measurement of these cultures corroborated our observations (Appendix Figure 4).

Despite the major ORF3b deletion, our results demonstrate that the wave 4 virus does not have an enhanced ability to replicate ex vivo and retains potent innate immune evasion capacity in our experimental models. We noted that the wave 3 virus replicates slightly better than isolates from wave 1 and 4, and it can induce higher innate immune responses. The wave 3 virus has several unique mutations not found in the other 2 viruses (Table). Many of these mutations are in the ORF1ab or N gene. Although not within the scope of this study, further characterization of mutations found in the wave 3 virus via reverse genetics (*9*) might help explain our observations.

### Conclusion

In summary, we found the virus causing the fourth COVID-19 epidemic wave in Hong Kong does not have enhanced replication kinetics and is not a potent cytokine or chemokine inducer. However, our work highlights the need for stringent COVID-19 control policy in quarantine settings.

### Acknowledgments

We gratefully acknowledge the staff from the originating laboratories responsible for obtaining the specimens and from the submitting laboratories where the genome data were generated and shared via GISAID (Appendix Table 2). We thank the following for providing technical support: Rachel H.H. Ching and John C.W. Ho from the School of Public Health, the University of Hong Kong; Kevin Fung from the Pathology Department of the University of Hong Kong; and colleagues from the Centre for PanorOmic Sciences of the University of Hong Kong.

This work is supported by grants from the National Institute of Allergy and Infectious Diseases (contract no. HHSN272201400006C), Research Grant Council of Hong Kong (no. T11-712/19-N), and the Health and Medical Research Fund (grant nos. COVID190205 and COVID190202).

## About the Author

Dr. Chu is a research assistant professor at The University of Hong Kong, Hong Kong. His interests focus on diagnostic virology, molecular diagnostics, and virus evolution.

### References

1. Siu GK, Lee LK, Leung KS, Leung JS, Ng TT, Chan CT, et al. Will a new clade of SARS-CoV-2 imported into the community spark a fourth wave of the COVID-19 outbreak in Hong Kong? Emerg Microbes Infect. 2020;9:2497–500. https://doi.org/10.1080/22221751.2020.1851146
2. Choi EM, Chu DKW, Cheng PKC, Tsang DNC, Peiris M, Bausch DG, et al. In-flight transmission of SARS-CoV-2. Emerg Infect Dis. 2020;26:2713–6. https://doi.org/10.3201/eid2611.203254
3. Sit THC, Brackman CJ, Ip SM, Tam KWS, Law PYT, To EMW, et al. Infection of dogs with SARS-CoV-2. Nature. 2020;586:776–8. https://doi.org/10.1038/s41586-020-2334-5
4. Garvin MR, Prates ET, Pavicic M, Jones P, Amos BK, Geiger A, et al. Potentially adaptive SARS-CoV-2 mutations discovered with novel spatiotemporal and explainable AI models. Genome Biol. 2020;21:304. https://doi.org/10.1186/s13059-020-02191-0
5. Xia H, Cao Z, Xie X, Zhang X, Chen JY, Wang H, et al. Evasion of type I interferon by SARS-CoV-2. Cell Rep. 2020;33:108234. https://doi.org/10.1016/j.celrep.2020.108234
6. Lam JY, Yuen CK, Ip JD, Wong WM, To KK, Yuen KY, et al. Loss of orf3b in the circulating SARS-CoV-2 strains. Emerg Microbes Infect. 2020;9:2685–96. https://doi.org/10.1080/22221751.2020.1852892
7. Hui KPY, Cheung MC, Perera RAPM, Ng KC, Bui CHT, Ho JCW, et al. Tropism, replication competence, and innate immune responses of the coronavirus SARS-CoV-2 in human respiratory tract and conjunctiva: an analysis in ex-vivo and in-vitro cultures. Lancet Respir Med. 2020;8:687–95. https://doi.org/10.1016/S2213-2600(20)30193-4
8. Hui KPY, Ching RHH, Chan SKH, Nicholls JM, Sachs N, Clevers H, et al. Tropism, replication competence, and innate immune responses of influenza virus: an analysis of human airway organoids and ex-vivo bronchus cultures. Lancet Respir Med. 2018;6:846–54. https://doi.org/10.1016/S2213-2600(18)30236-4
9. Thi Nhu Thao T, Labroussaa F, Ebert N, V'kovski P, Stalder H, Portmann J, et al. Rapid reconstruction of SARS-CoV-2 using a synthetic genomics platform. Nature. 2020;582:561–5. https://doi.org/10.1038/s41586-020-2294-9

Addresses for correspondence: Michael Chan or Leo Poon, School of Public Health, G/F Patrick Manson Building (North Wing), University of Hong Kong, 7 Sassoon Road, Pokfulam, Hong Kong, China; email: mchan@hku.hk or llmpoon@hku.hk

Article DOI: https://doi.org/10.3201/eid2705.210015

# Introduction of ORF3a-Q57H SARS-CoV-2 Variant Causing Fourth Epidemic Wave of COVID-19, Hong Kong, China

## Appendix

## Additional Methods

### Quarantine Policy and Testing Strategy for Inbound Travelers

Inbound travelers arriving by air were tested by reverse transcription-PCR (RT-PCR) for severe acute respiratory syndrome coronavirus 2 (SARS-CoV-2) upon arrival at Hong Kong International Airport. Travelers were mandated to wait for results at the testing site in the airport. Positive coronavirus disease (COVID-19) cases were sent to a hospital for treatment, but negative cases stayed in a designated hotel for a 14-day compulsory quarantine. On day 12 of their quarantine period, quarantined travelers were instructed to provide samples for an additional RT-PCR test. All the RNA samples were tested in a World Health Organization (WHO) Reference Laboratory in the Public Health Laboratory Centre, Hong Kong. Current quarantine policy is available from https://www.coronavirus.gov.hk/eng/inbound-travel-faq.html.

### Investigation of Local Cases

The investigation of local cases was initiated by the detection of an index case in each of the local clusters. Active contact tracing investigations were immediately conducted by the Hong Kong Government thereafter. Persons epidemiologically linked to these clusters (e.g., close contacts) were required to provide respiratory samples for COVID-19 RT-PCR tests. All epidemiologic data described in the manuscript were retrieved from public datasets (https://data.gov.hk/en-daata/dataset/hk-dh-chpsebcddr-novel-infectious-agent).

### Sequencing

RNA samples for our study were sent to a WHO reference laboratory at the University of Hong Kong for full genome analyses (IRB no. UW 20–168). We deduced near full-length genomes from all available samples, patients BB1–BB13 and patients C1–C9, with sequence

length >29,700 nt and sequence coverage >100 by using an Illumina (https://www.illumina.com) sequencing protocol we described previously (*1*). In brief, virus genome was reverse transcribed with multiple gene-specific primers targeting different regions of the viral genome. The synthesized cDNA was then subjected to multiple overlapping 2-kb PCRs for full-genome amplification. PCR amplicons obtained from the same specimen were pooled and sequenced by using Nova sequencing platform (Illumina). Sequencing library was prepared by using Nextera XT (Illumina).

### Phylogenetic Analysis

Generated sequencing reads were mapped to a reference virus genome by BWA (http://bio-bwa.sourceforge.net), and genome consensus was generated by Geneious version 11.1.4 (https://www.geneious.com). Sequences from each phylogenetic clade (G, GH, GR, L, O, S, and V) of SARS-CoV-2 were selected from GISAID for phylogenetic analysis (Appendix Table 2). Viral sequences were aligned by using BioEdit (https://www.bioedit.com) and phylogenetically analyzed by using MEGA-X (https://www.megasoftware.net). We constructed the phylogenetic tree by using the neighbor-joining method with 500 bootstraps.

### Virus Isolates Used in Characterization

Virus isolated from the wave 1 (clade L), wave 3 (clade GR), and wave 4 (clade GH) of COVID-19 in Hong Kong were used for phenotypic characterization. The wave 1 virus was isolated from an imported case identified in a 39-year-old symptomatic man, as previously described (*2*). The wave 3 virus was isolated from a locally transmitted case in a 57-year-old symptomatic woman. The wave 4 virus was isolated from patient A2 in this study, a 43-year-old asymptomatic man. These patients recovered and were discharged from hospital.

### Ex Vivo Cultures and Infection of Human Respiratory Tract

Infection procedures were performed as previously described (*2*). In brief, nontumor bronchus and lung tissues were obtained from patients undergoing elective surgery, as detailed previously (*3*,*4*). Fragments of human tissues were infected with each virus at $5 \times 10^5$ $TCID_{50}$/mL for 1 h at 37°C. The explants were washed 3 times with phosphate buffered saline (PBS) and placed in culture medium (F-12K nutrient mixture with L-glutamine and antibiotics) and incubated at 37°C with 5% $CO_2$. Infectious viral titers in culture supernatants were assessed at 1 h, 24 h, 48 h, 72 h, and 96 h post-infection (hpi) by titration in Vero E6 cells. One set of

bronchus and lung tissues were fixed at 96 hpi in 10% formalin and processed for immunohistochemistry staining.

### 2-Dimensional Differentiated Human Airway Organoid Culture and Infection

The human airway organoids were established from human lung tissues, as previously described (*5*). The 2-dimensional differentiated airway organoid model was further built on the airway organoids, as previously described (*6*), with a few modifications. In brief, airway organoids were dissociated into single cells using TrypLE select (GIBCO, https://www.thermofisher.com) for 10 min at 37°C. The digest was then sheared by using 25-gauge needle and strained over a 40 μm cell strainer. We seeded 150,000 cells onto Transwell insert (Corning, https://www.corning.com) pre-coated with rat tail collagen 1 (Corning). The cells were cultured in a mixture of airway organoid growth medium (*5*) and Pneumacult-ALI (Stemcell, https://www.stemcell.com) complete base medium at a ratio of 1:1 at 37°C for 3–4 days. Once the cells reached confluency, they were cultured at air-liquid interface (ALI) in Pneumacult-ALI Maintenance Medium (Stemcell). The medium was changed every 3 days. The 2-dimensional transwell cultures were used for infection after 3 weeks of differentiation. Cells were infected with the coronaviruses at a multiplicity of infection of 2 at the apical side for 1 h at 37°C. Cells were washed with PBS and culture at ALI in the same growth medium.

### Viral Titration by $TCID_{50}$ assay

Vero-E6 cells were seeded on 96-well tissue culture plates 1 day before the virus titration ($TCID_{50}$) assay. Cells were washed once with PBS and replenished with 2% DMEM medium supplemented with 100 units/mL of penicillin and 100 μg/mL of streptomycin. Serial dilutions of virus supernatant, from 0.5–7 log, were performed before adding the virus dilutions onto the plates in quadruplicate. The plates were observed daily for cytopathic effects. The endpoint of viral dilution leading to CPE in 50% of inoculated wells was estimated by using the Karber method (*7*). Area-under-curve (AUC) was calculated by integrating infectious virus titers at 24–96 hpi in ex vivo bronchus and lung tissues.

### Immunohistochemical Staining

Immunohistochemical staining of the respiratory tract tissue was carried out for the SARS-CoV-2 nucleoprotein, as previously described (*2*). The fixed paraffin-embedded ex vivo cultures of human tissues were stained with SARS-CoV nucleoprotein (4D11) (*4*,*5*,*8*). The tissue

sections were first microwaved in 10 mmol citrate buffer, blocked with 10% normal horse serum at room temperature. The sections were then incubated with 4D11 antibody followed by alkaline phosphatase (AP) conjugated antimouse antibody (Vector Laboratories, Inc., https://vectorlabs.com ) and developed with VectorRed (VR) (Vector Laboratories, Inc.).

### Real-time PCR assay

The RNA of infected cells were extracted at 48 h post infection by using a MiniBEST Universal RNA Extraction Kit (TaKaRa Bio, Inc., http://www.takara-bio.com). RNA was reverse-transcribed by using Oligo-dT primers with Advantage RT-for-PCR Kit (TaKaRa Bio, Inc.). mRNA expression of target genes was performed by using ViiA7 Real-Time PCR System (Applied Biosystems, https://www.thermofisher.com). The gene expression profiles were quantified and normalized with β-actin, as previously described (*9*–*11*).

### Cytometric Bead Array

Protein concentration of interferon gamma-induced protein-10 in the supernatants collected from apical and basolateral chambers was determined by bead-based immunoassays, BD Cytometric Bead Array (BD Bioscience, https://www.bdbiosciences.com) according to the manufacturer's protocol. In brief, 50 μL of cell culture supernatant and a 10-point standard curve (ranging from 0–2,500 pg/mL) was used for the measurement of each cytokine and chemokine. The samples were analyzed by using a BD LSR Fortessa Analyzer (BD Bioscience). Standard curves for the cytokines and chemokines were built and the fluorescence intensity concentrations were calculated by using FlowJo version 7.6.1 (https://www.flowjo.com).

### Biosafety and Ethics

All infection work was carried out in a Biosafety Level-3 facility. Informed consent was obtained from all subjects and approval was granted by the Institutional Review Board of the University of Hong Kong and the Hospital Authority (Hong Kong West) (approval no. UW 20–167).

### References

1. Sit THC, Brackman CJ, Ip SM, Tam KWS, Law PYT, To EMW, et al. Infection of dogs with SARS-CoV-2. Nature. 2020;586:776–8. PubMed https://doi.org/10.1038/s41586-020-2334-5

2. Hui KPY, Cheung MC, Perera RAPM, Ng KC, Bui CHT, Ho JCW, et al. Tropism, replication competence, and innate immune responses of the coronavirus SARS-CoV-2 in human respiratory tract and conjunctiva: an analysis in ex-vivo and in-vitro cultures. Lancet Respir Med. 2020;8:687–95. PubMed https://doi.org/10.1016/S2213-2600(20)30193-4

3. Chan MC, Chan RW, Yu WC, Ho CC, Yuen KM, Fong JH, et al. Tropism and innate host responses of the 2009 pandemic H1N1 influenza virus in ex vivo and in vitro cultures of human conjunctiva and respiratory tract. Am J Pathol. 2010;176:1828–40. PubMed https://doi.org/10.2353/ajpath.2010.091087

4. Hui KP, Chan LL, Kuok DI, Mok CK, Yang ZF, Li RF, et al. Tropism and innate host responses of influenza A/H5N6 virus: an analysis of ex vivo and in vitro cultures of the human respiratory tract. Eur Respir J. 2017;49:1601710. PubMed https://doi.org/10.1183/13993003.01710-2016

5. Hui KPY, Ching RHH, Chan SKH, Nicholls JM, Sachs N, Clevers H, et al. Tropism, replication competence, and innate immune responses of influenza virus: an analysis of human airway organoids and ex-vivo bronchus cultures. Lancet Respir Med. 2018;6:846–54. PubMed https://doi.org/10.1016/S2213-2600(18)30236-4

6. Lamers MM, Beumer J, van der Vaart J, Knoops K, Puschhof J, Breugem TI, et al. SARS-CoV-2 productively infects human gut enterocytes. Science. 2020;369;50–4. PubMed https://doi.org/10.1126/science.abc1669

7. Karber G. 50% end-point calculation. Arch Exp Pathol Pharmak. 1931;162:480–3.

8. Nicholls JM, Butany J, Poon LL, Chan KH, Beh SL, Poutanen S, et al. Time course and cellular localization of SARS-CoV nucleoprotein and RNA in lungs from fatal cases of SARS. PLoS Med. 2006;3:e27. PubMed https://doi.org/10.1371/journal.pmed.0030027

9. Chan RW, Chan MC, Wong AC, Karamanska R, Dell A, Haslam SM, et al. DAS181 inhibits H5N1 influenza virus infection of human lung tissues. Antimicrob Agents Chemother. 2009;53:3935–41. PubMed https://doi.org/10.1128/AAC.00389-09

10. Hui KP, Lee SM, Cheung CY, Mao H, Lai AK, Chan RW, et al. H5N1 influenza virus-induced mediators upregulate RIG-I in uninfected cells by paracrine effects contributing to amplified cytokine cascades. J Infect Dis. 2011;204:1866–78. PubMed https://doi.org/10.1093/infdis/jir665

11. Hui KP, Lee SM, Cheung CY, Ng IH, Poon LL, Guan Y, et al. Induction of proinflammatory cytokines in primary human macrophages by influenza A virus (H5N1) is selectively regulated by IFN regulatory factor 3 and p38 MAPK. J Immunol. 2009;182:1088–98. PubMed https://doi.org/10.4049/jimmunol.182.2.1088

**Appendix Table 1.** Cases causing the fourth wave of coronavirus disease, Hong Kong

| Cluster | Patient | Date RT-PCR–confirmed |
|---|---|---|
| Hotel A | A1* | 20 Sep 2020 |
| Hotel A | A2* | 20 Sep 2020 |
| Hotel A | A3* | 20 Sep 2020 |
| Hotel A | A4* | 4 Oct 2020 |
| Hotel B | B1* | 20 Sep 2020 |
| Hotel B | B2* | 20 Sep 2020 |
| Bar/Build X | BB1* | 1 Oct 2020 |
| Bar/Build X | BB2* | 3 Oct 2020 |
| Bar/Build X | BB3* | 4 Oct 2020 |
| Bar/Build X | BB4 | 4 Oct 2020 |
| Bar/Build X | BB5* | 5 Oct 2020 |
| Bar/Build X | BB6* | 6 Oct 2020 |
| Bar/Build X | BB7* | 7 Oct 2020 |
| Bar/Build X | BB8* | 7 Oct 2020 |
| Bar/Build X | BB9* | 7 Oct 2020 |
| Bar/Build X | BB10* | 8 Oct 2020 |
| Bar/Build X | BB11* | 9 Oct 2020 |
| Bar/Build X | BB12* | 10 Oct 2020 |
| Bar/Build X | BB13* | 11 Oct 2020 |
| Bar/Build X | BB14 | 12 Oct 2020 |
| Bar/Build X | BB15 | 13 Oct 2020 |
| Hotel C | C1* | 6 Oct 2020 |
| Hotel C | C2* | 9 Oct 2020 |
| Hotel C | C3* | 9 Oct 2020 |
| Hotel C | C4* | 9 Oct 2020 |
| Hotel C | C5* | 9 Oct 2020 |
| Hotel C | C6* | 10 Oct 2020 |
| Hotel C | C7* | 12 Oct 2020 |
| Hotel C | C8* | 18 Oct 2020 |
| Hotel C | C9* | 19 Oct 2020 |

*Sequenced samples

**Appendix Table 2.** Names, accession numbers, and submission dates of severe acute respiratory syndrome coronavirus 2 genomes deposited in GISAID and used in a study of outbreaks in the fourth wave of coronavirus disease, Hong Kong

| Virus name | Accession No. | Date collected 2020 | Originating laboratory | Submitting laboratory | Authors |
|---|---|---|---|---|---|
| Australia/VIC1158/2020 | EPI_ISL_430602 | 9 Apr | Victorian Infectious Diseases Reference Laboratory (VIDRL) | Microbiological Diagnostic Unit Public Health Laboratory and Victorian Infectious Diseases Reference Laboratory, The Peter Doherty Institute for Infection and Immunity | L. Caly et al. |
| Australia/VIC1787/2020 | EPI_ISL_456649 | 27 May | Victorian Infectious Diseases Reference Laboratory (VIDRL) | Microbiological Diagnostic Unit Public Health Laboratory and Victorian Infectious Diseases Reference Laboratory, Doherty Institute | Caly et al. |
| Australia/VIC98/2020 | EPI_ISL_419810 | 16 Mar | Victorian Infectious Diseases Reference Laboratory (VIDRL) | Victorian Infectious Diseases Reference Laboratory and Microbiological Diagnostic Unit Public Health Laboratory, Doherty Institute | Caly et al. |
| England/20132080404/2020 | EPI_ISL_423805 | 24 Mar | Respiratory Virus Unit, Microbiology Services Colindale, Public Health England | Respiratory Virus Unit, Microbiology Services Colindale, Public Health England | M. Galiano et al. |
| England/CAMB-77909/2020 | EPI_ISL_439431 | 31 Mar | Department of Pathology, University of Cambridge | Wellcome Sanger Institute for the COVID-19 Genomics UK (COG-UK) consortium | L.W. Meredith et al. |
| England/NORW-EC85D/2020 | EPI_ISL_457566 | 13 May | Quadram Institute Bioscience | COVID-19 Genomics UK (COG-UK) Consortium | D.J. Baker et al. |
| England/SHEF-C03E5/2020 | EPI_ISL_420221 | 29 Mar | Virology Department, Sheffield Teaching Hospitals NHS Foundation Trust | Department of Infection, Immunity and Cardiovascular Disease, The Florey Institute, The Medical School, University of Sheffield | Thushan de Silva et al. |
| France/HDF-3668/2020 | EPI_ISL_443316 | 25 Mar | CH CompiÃgne Laboratoire de Biologie | National Reference Center for Viruses of Respiratory Infections, Institut Pasteur, Paris | M. Albert et al. |
| HongKong/VB20175856/2020 | EPI_ISL_539823 | 14 Aug | Communicable Disease Branch | Hong Kong Department of Health | Alan K.L. Tsang et al |
| HongKong/VM20066524/2020 | EPI_ISL_539814 | 21 Jul | Tuen Mun Hospital | Hong Kong Department of Health | A.K.L. Tsang et al. |
| Iceland/99/2020 | EPI_ISL_417768 | 10 Mar | The National University Hospital of Iceland | deCODE genetics | D.F. Gudbjartsson et al. |
| India/GJ-GBRC137b/2020 | EPI_ISL_458095 | 24 May | B.J. Medical College and Civil hospital | Gujarat Biotechnology Research Centre | R. Kumar et al. |
| India/OR-RMRC164/2020 | EPI_ISL_455764 | 7 May | REGIONAL VRDL, ICMR-RMRC BBSR | Immunogenomics lab, Institute of Life Sciences, Bhubaneswar | S. Raghav et al. |
| Japan/Hu_DP_Kng_19–031/2020 | EPI_ISL_420889 | 14 Feb | Takayuki Hishiki Kanagawa Prefectural Institute of Public Health | Takayuki Hishiki Kanagawa Prefectural Institute of Public Health | Hishiki et al. |
| Nepal/2097/2020 | EPI_ISL_754068 | 30 Jul | Nepal Korea Friendship Municipality Hospital | Nepal Health Research Council | P. Gyanwali et al. |
| Nepal/2178/2020 | EPI_ISL_754069 | 31 Jul | Nepal Korea Friendship Municipality Hospital | Nepal Health Research Council | P. Gyanwali et al. |
| Nepal/2673/2020 | EPI_ISL_754070 | 7 Aug | Nepal Korea Friendship Municipality Hospital | Nepal Health Research Council | P. Gyanwali et al. |
| Nepal/459A/2020 | EPI_ISL_754072 | 3 Aug | National Public Health Laboratory | Nepal Health Research Council | P. Gyanwali et al. |
| Nepal/61/2020 | EPI_ISL_410301 | 13 Jan | National Influenza Centre, National Public Health Laboratory, Kathmandu, Nepal | The University of Hong Kong | R. Sah et al. |

| Virus name | Accession No. | Date collected 2020 | Originating laboratory | Submitting laboratory | Authors |
|---|---|---|---|---|---|
| Nepal/614/2020 | EPI_ISL_754062 | 7 Aug | Kathmandu University | Nepal Health Research Council | P. Gyanwali et al. |
| Nepal/616/2020 | EPI_ISL_754063 | 10 Aug | Kathmandu University | Nepal Health Research Council | P. Gyanwali et al. |
| Nepal/617/2020 | EPI_ISL_754064 | 10 Aug | Kathmandu University | Nepal Health Research Council | P. Gyanwali et al. |
| Nepal/618/2020 | EPI_ISL_754065 | 10 Aug | Kathmandu University | Nepal Health Research Council | P. Gyanwali et al. |
| Nepal/619/2020 | EPI_ISL_754066 | 10 Aug | Kathmandu University | Nepal Health Research Council | P. Gyanwali et al. |
| Nepal/620/2020 | EPI_ISL_754067 | 9 Aug | Kathmandu University | Nepal Health Research Council | P. Gyanwali et al. |
| Nepal/70N/2020 | EPI_ISL_754073 | 3 Aug | National Public Health Laboratory | Nepal Health Research Council | P. Gyanwali et al. |
| Nepal/962/2020 | EPI_ISL_754060 | 3 Aug | National Public Health Laboratory | Nepal Health Research Council | P. Gyanwali et al. |
| Nepal/C3031/2020 | EPI_ISL_754071 | 10 Aug | Nepal Korea Friendship Municipality Hospital | Nepal Health Research Council | P. Gyanwali et al. |
| Nepal/H353/2020 | EPI_ISL_754061 | 3 Aug | National Public Health Laboratory | Nepal Health Research Council | P. Gyanwali et al. |
| NewZealand/20VR3045/2020 | EPI_ISL_456402 | 25 Apr | Wellington SCL | Institute of Environmental Science and Research (ESR) | M. Storey et al. |
| Portugal/PT0163/2020 | EPI_ISL_453879 | 28 Mar | Unknown | Instituto Nacional de Saude (INSA) | Borges et al. |
| Spain/MD-ISCIII-201738/2020 | EPI_ISL_419237 | 7 Mar | Fundacion Jimenez Diaz | Instituto de Salud Carlos III | Iglesias-Caballero et al. |
| USA/CA-CZB-1237/2020 | EPI_ISL_454657 | 12 May | County of Santa Clara Public Health Department | Chan-Zuckerberg Biohub | CZB Cliahub Consortium et al. |
| Wales/PHWC-3180E/2020 | EPI_ISL_446492 | 11 Apr | Wales Specialist Virology Centre | Public Health Wales Microbiology Cardiff | C. Moore et al. |
| Wales/PHWC-32B6E/2020 | EPI_ISL_446656 | 14 Apr | Wales Specialist Virology Centre | Public Health Wales Microbiology Cardiff | C. Moore et al. |
| Wuhan/HB-WH1–131/2020 | EPI_ISL_454910 | 2 Mar | Wuhan Chain Medical Labs (CMLabs) | State Key Laboratory of Biotherapy of Sichuan University | B. Du et al. |
| Wuhan/WIV04/2019 | EPI_ISL_402124 | 30 Dec 2019 | Wuhan Jinyintan Hospital | Wuhan Institute of Virology, Chinese Academy of Sciences | P. Zhou et al. |

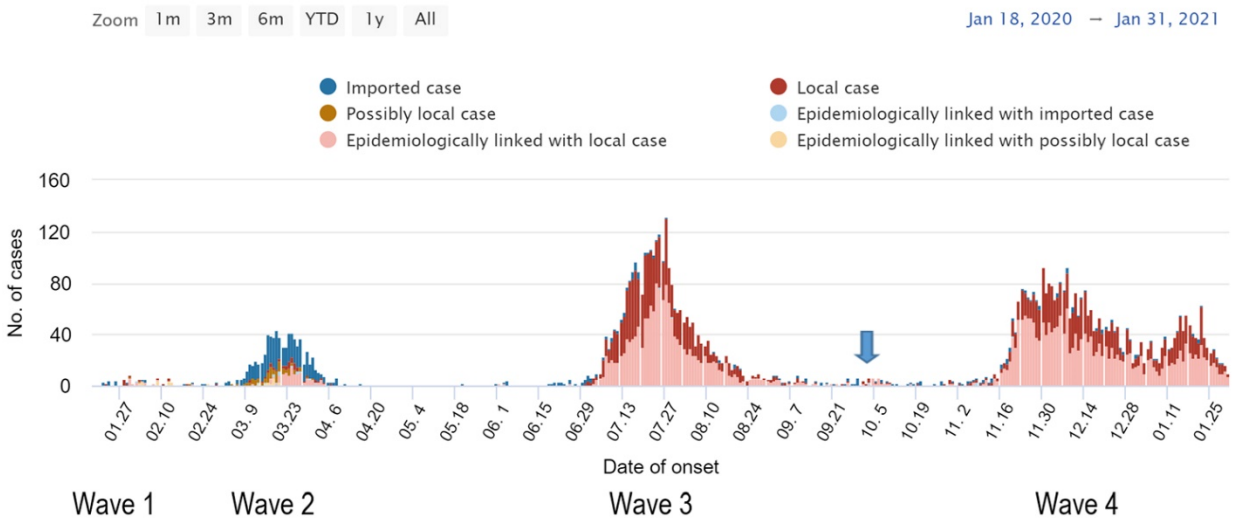


**Appendix Figure 1.** Coronavirus disease epidemic waves, Hong Kong, China. Hong Kong experienced 4 waves of COVID-19. The number of cases per day are show with differential epidemiologic links are indicated. Blue arrow indicates outbreaks in bar/building X and hotel C. Data were extracted from https://covid19.sph.hku.hk.

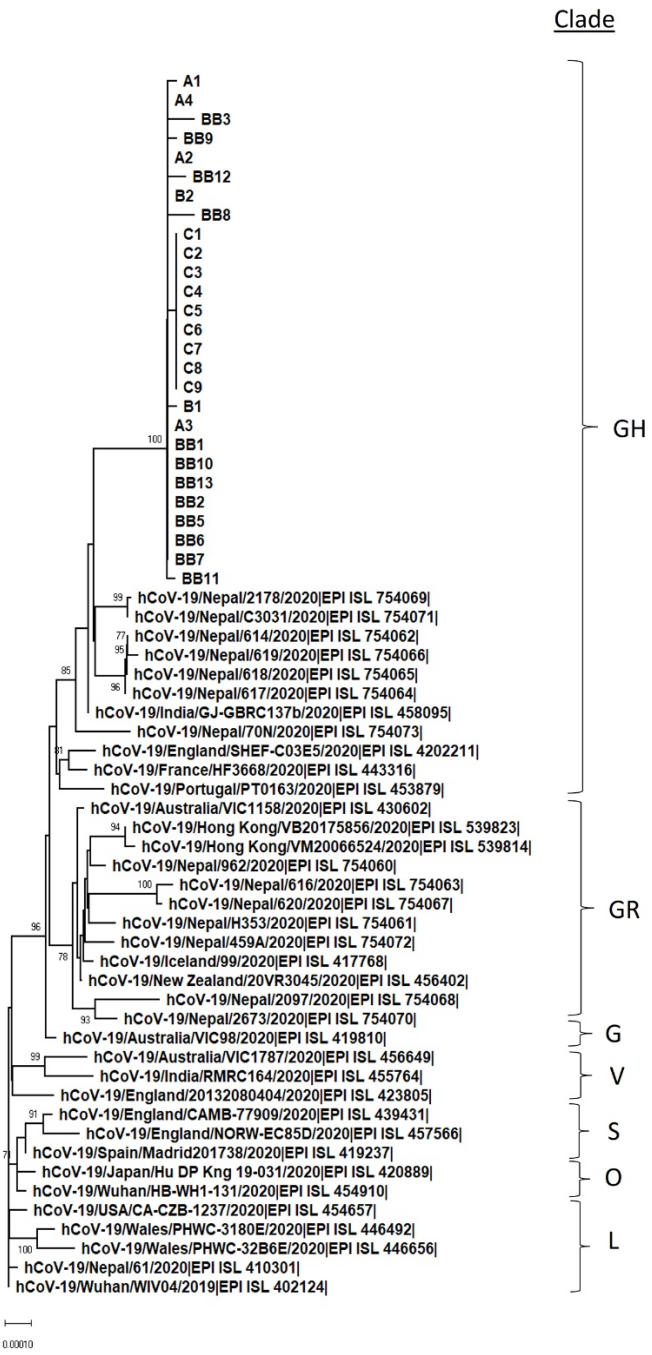


**Appendix Figure 2.** Phylogenetic tree of the SARS-CoV-2 detected in COVID-19 cases causing the fourth epidemic wave, Hong Kong, China. We used human SARS-CoV-2 WIV04 as the root of this phylogenetic tree. The tree was constructed by using the neighbor-joining method. Only bootstrap values >70 are shown. Viruses from clades L, S, V, G, GH, GR, and O (others) are included in the analysis. EPI ISL accession nos. for sequences were retrieved from GISAID (https://platform.gisaid.org). Scale bar indicates estimated genetic distance. COVID-19, coronavirus disease. SARS-CoV-2, severe acute respiratory syndrome coronavirus 2.

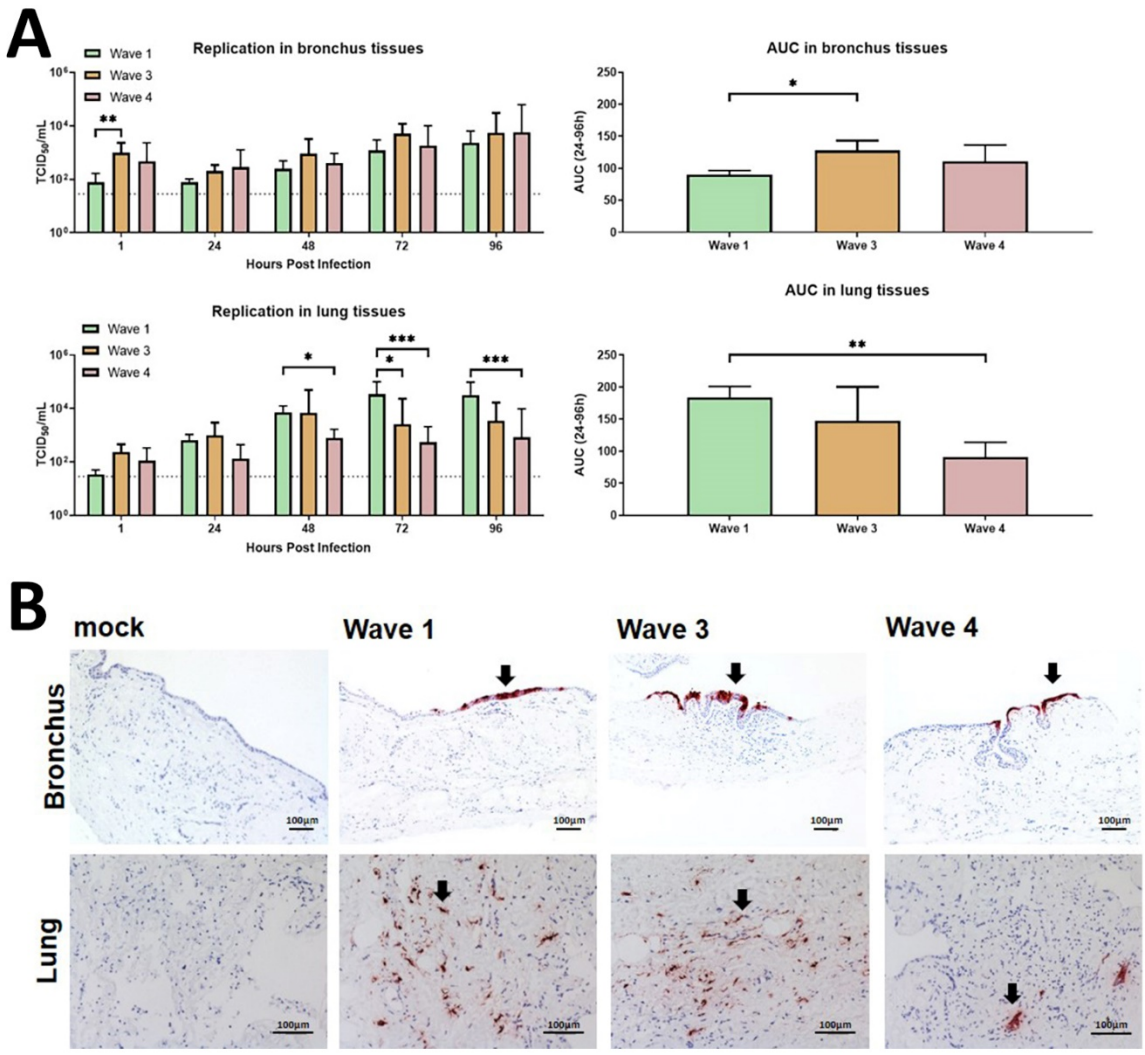


**Appendix Figure 3.** Viral replication kinetics of wave 1, 3, and 4 SARS-CoV-2 viruses in ex vivo cultures of human respiratory tract tissues. Human ex vivo cultures of bronchus (n = 4) and lung (n = 3), were infected with $5 \times 10^5$ $TCID_{50}$/mL at 37°C. Culture supernatants were harvested at the indicated times and virus titers were measured by $TCID_{50}$ assay. A) Bar-charts show the mean virus titer $\pm$ SD. The horizontal dotted line denotes the limit of detection in the $TCID_{50}$ assay. Area-under-curve (AUC) was calculated from the viral titers from 24h to 96h. Bar charts of AUC show the mean $\pm$ SD. The differences between viral titers were compared using 2-way ANOVA followed by a Tukey multiple-comparison test. The differences of AUC between viruses were compared using 1-way ANOVA followed by a Tukey multiple-comparison test. *p<0.05; **p<0.01; ***p<0.001. B) Mock and infected tissues formalin-fixed at 96 h post infection. Top row, bronchi; bottom row, lung. Paraffin embedded sections were subjected to immunohistochemical staining with a monoclonal antibody against the SARS-CoV-2 NP. Arrows indicate positive cells are in red. Magnification ×100 in bronchus tissues; magnification ×200 in lung tissues. Scale bar indicates 100 µm. NP, nucleoprotein; SARS-CoV-2, severe acute respiratory syndrome coronavirus 2; SD, standard deviation.

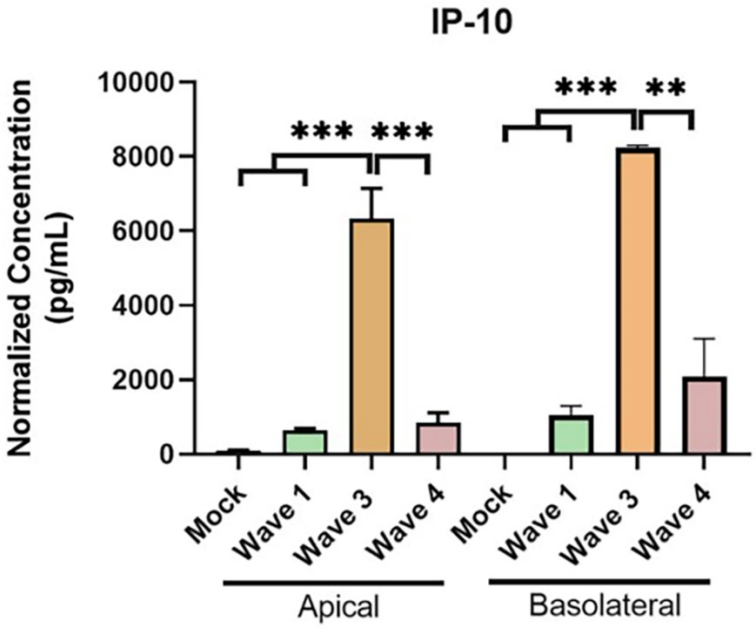


**Appendix Figure 4.** IP-10 expression in human airway organoids infected by wave 1, 3, or 4 SARS-CoV-2 virus, Hong Kong, China. At 48 h post infection, concentrations of IP-10 in the culture supernatants from both apical and basal chamber were measured by cytometric bead assay. The concentrations of infected cells were normalized with ORF1b gene. Results are the calculated mean from 2 independent experiments ± SD of mean. The differences were compared using 1-way ANOVA followed by a Tukey multiple-comparison test. Means and standard deviation error bars are as shown **p<0.01; ***p<0.001. IP-10, interferon gamma-induced protein-10 SARS-CoV-2, severe acute respiratory syndrome coronavirus 2.